Supporting Information

Silver et al. 10.1073/pnas.1006968107

SI Text

Euphotic-zone samples of oceanic phytoplankton were obtained from five oceanic expeditions (Fig. 1). Three of these were natural populations from the North Pacific, (GOA, VERTIGO K2, VERTIGO ALOHA), and two were populations that developed during mesoscale Fe-fertilization experiments in the Equatorial and Antarctic Pacific (IronEx II and SOFeX) (1–3). The data used in this study are presented in Table S1 and include sample identifiers, station, and geographic locations, *Pseudo-nitzschia* abundances, and cellular and water levels of DA. We also present dissolved Fe and nitrate, because we felt these would help to inform the discussion of *Pseudo-nitzschia* blooms in response to Fe fertilization of HNLC regions of the world's oceans.

SI Methods

Dissolved Nitrate and Iron. For the GOA samples, macronutrients (nitrite + nitrate; referred to herein as nitrate) concentrations were measured on a Lachat QuickChem 8000 Flow Injection Analysis system by using standard methods (4). The SE for nutrient measurements was within 2–3%. On the VERTIGO cruises, frozen water samples for the determination of nitrate and nitrite were analyzed at the shore laboratory with a Technicon Auto-Analyzer II by following the procedure of Hansen and Grasshof (5). The detection limit was ≈0.1 μmol·L^{-1} (6). During SOFeX, nitrate was analyzed by standard autoanalytical methods immediately onboard the ship (7). During IronEx II, surface nitrate contours were constructed from underway measurements from the ship's flow-through system by using an Alpkem segmented flow auto-analyzer. Calibrations with periodic standards and a daily series of discrete samples and standards were run on an independent analyzer (3).

Total dissolved iron was measured in the GOA and during Fe-enrichment experiments, IronEx II and SOFeX. For GOA, a combination of electrochemical (8), modified atomic absorption (9), or underway flow injection (10) methods were used. During IronEx II and SOFeX, underway measurements were made by using flow injection analysis with chemiluminescence detection (11). Detection limit for the combined system was 0.2 nM. Values were confirmed by electrochemical and modified atomic absorption methods (9).

Natural Abundances of *Pseudo-nitzschia* spp. in the Euphotic Zone. Cell counts were made on discrete water samples collected with Niskin bottles to determine the natural abundances of *Pseudo-nitzschia* at the surface, generally 10–30 m. In the case of the VERTIGO samples, additional samples were taken from deeper within the euphotic zone (ALOHA, 125 m; K2, 40 m). By integrating these abundances over the respective euphotic zones (Aloha, 160 m; K2, 60 m), *Pseudo-nitzschia* standing stocks were calculated from which euphotic zone abundances were derived. On the GOA, SOFeX, and IronEx II cruises, cell counts were made at sea as follows: Sample aliquots of 20–100 mL were filtered onto 0.8-μm Nuclepore filters, preserved with 2% glutaraldehyde, stained with 4′6-diamidino-2-phenylindole (DAPI) and counted on a Zeiss Axioscope (12). Counts were made by using a combination of transmitted light and epi-fluorescent microscopy. Counts on the VERTIGO samples were made on 50- to 100-mL preserved (4% hexamine buffered formalin) and DAPI-stained aliquots back in the shore laboratory by using the Utermöhl method (13). Counts were made on an Olympus IX 70 inverted microscope or Olympus BH-2 by using a combination of transmitted light and epi-fluorescent microscopy. Only pennate cells in stepped-chains, characteristic of the genus *Pseudo-nitzschia*, and containing protoplasm, were counted. Empty frustules and single cells were not counted, so abundance estimates are conservative. At least 400 cells or the entire settled volume of 50 mL was counted. The detection limit by these methods was 20 cells·L^{-1}.

Daily *Pseudo-nitzschia* Fluxes in the Mesopelagic Zone. During the two VERTIGO cruises, at stations ALOHA and K2, we obtained samples of sinking particulate matter from four separate deployments, using neutrally buoyant sediment traps (1) (Table 3). Each 3–5 d deployment consisted of replicate traps deployed at three subeuphotic depths: 150, 300, and 500 m. Immediately after retrieval, samples were gravity filtered through a 350-μm screen to remove large zooplankton and wet-split into eight subfractions that were subsequently preserved in 4% hexamine buffered formalin. Two subfractions were dedicated to *Pseudo-nitzschia* cell counts, carried out as described above for the settled water samples. By knowing the deployment duration and the trap surface collection area, we estimated the delivery rate of *Pseudo-nitzschia* cells to the mesopelagic zone (as cells·m^{-2}·d^{-1}) (1). Again, only cells with intact protoplasts were counted, i.e., those that were presumably living or recently live. By dividing this flux estimate by the integrated *Pseudo-nitzschia* cell population (standing stock) in the overlying euphotic zone, we estimated the percentage of the surface standing stock of *Pseudo-nitzschia* that reached trap depths on a daily basis.

Electron Microscopy: *Pseudo-Nitzschia* spp. Studies. Both scanning (SEM) and transmission (TEM) electron microscopy were used on the natural mixes of phytoplankton from net tows, using methods slightly modified from the literature (14, 15). All micrographs were obtained with a Cambridge Stereoscan 260 scanning electron microscope at 10 kV. For TEM analysis of the frustules, a drop of cleaned material was pipetted onto a copper grid (mesh size 100), a mesh size with Formvar coating and stabilized with an evaporated carbon film. The grids were left to air-dry and then viewed with a JEOL 100-CX transmission electron microscope. The morphometrics of the features used for making the identifications are presented in Table S2.

cELISA Assay for Domoic Acid. The cELISA is based on the detection of DA by specific antibodies in a direct competition format, where free DA in the sample competes for binding to the specific antibodies with DA-conjugated proteins. DA was measured routinely by using the high-sensitivity Biosense cELISA kits, using protocols provided by the manufacturer (16, 17). cELISA measures both DA and, to some extent, its isomers. We chose cELISA rather than HPLC methods for routine measurements because of the higher sensitivity of the former and its ability to measure DA in formalin-fixed samples (HPLC, in contrast, cannot accurately measure DA in samples preserved with formalin; ref. 16 and 17). Each sample was run in duplicate and at several dilutions. The color intensity was read by using a standard microplate absorbance reader at 450 nm. A calibration curve was generated by using the DA standard (National Research Council Canada, NRC CRM-DAe) provided in the cELISA kit, with concentrations including 0 (blank), 0.16, 0.56, 1.9, 6.5, 22, 75, 254, 865, 2,941, and 10,000 pg of DA·mL^{-1}.

SI Results

Relationship Between Domoic Acid Concentrations and *Pseudo-nitzschia*. Using the data from Table S1, we show the linear relationship between DA (expressed as DA mL^{-1} and total (intact)

cells (all species of this pennate genus) in Fig. S1. The relationship is highly significant ($P < 0.001$), and the cell abundance clearly explains most of the variation in the measured DA in the water. This statistic strongly suggests that processes that promote the growth and enhance the abundance of *Pseudonitschia* will also lead to high concentrations of domoic acid in the water.

1. Buessler KO, et al. (2008) VERTIGO (VERtical Transport in the Global Ocean): A study of particle sources and flux attenuation in the North Pacific. *Deep Sea Res Part II Top Stud Oceanogr* 55:1522–1539.
2. Coale KH, et al. (2004) Southern Ocean iron enrichment experiment: Carbon cycling in high- and low-Si waters. *Science* 304:408–414.
3. Coale KH, et al. (1996) A massive phytoplankton bloom induced by an ecosystem-scale iron fertilization experiment in the equatorial Pacific Ocean. *Nature* 383: 495–501.
4. Parsons TR, Maita Y, Lalli CM (1984) *A Manual of Chemical and Biological Methods for Seawater Analysis* (Pergamon, Oxford), p 173.
5. Hansen HP, Grasshoff K (2008) Automated Chemical Analysis. *Methods of Sea Water Analysis*, eds Grasshoff K, Ehrhardt M, Kremling K (Verlag Chemie, Weinheim, Germany), 2nd ed, pp 368–376.
6. Elskens M, et al. (2008) Primary, new and export production in the NW Pacific subarctic gyre during the vertigo K2 experiments. *Deep Sea Res Part II Top Stud Oceanogr* 55:1594–1604.
7. Gordon LI, Jennings JC Jr, Ross AA, Krest JM (1994) A Suggested Protocol for Continuous Flow Automated Analysis of Seawater Nutrients (Phosphate, Nitrate, Nitrite and Silicic Acid) in the WOCE Hydrographic Program and the Joint Global Ocean Fluxes Study. *WOCE Operations Manual* (Woods Hole Oceanographic Institution, Woods Hole, MA) WOCE report no. 68/91, revision 1, WHP Office Report WHPO91-1.
8. Rue EL, Bruland KW (1997) The role of organic complexation on ambient iron chemistry in the equatorial Pacific ocean and the response of a mesoscale iron addition experiment. *Limnol Oceanogr* 42:901–910.
9. Bruland K, Franks RP, Knauer GA, Martin JH (1979) Sampling and analytical methods for the determination of copper, cadmium, zinc, and nickel at the nanogram per liter level in sea water. *Anal Chim Acta* 105:233–245.
10. Lohan MC, Aguilar-Islas AM, Bruland KW (2006) Direct determination of iron in acidified (pH 1.7) seawater samples by flow injection analysis with catalytic spectrophotometric detection: Application and intercomparison. *Limnol Oceanogr Methods* 4:164–171.
11. Obata H, Karatani H, Nakayama E (1994) Automated determination of iron in seawater by chelating resin concentration and chemiluminescence detection. *Anal Chem* 65:1524–1528.
12. Landry ME, et al. (2000) Biological response to iron fertilization in the eastern equatorial Pacific (IronEx II). I. Microplankton community abundances and biomass. *Mar Ecol Prog Ser* 201:27–42.
13. Utermöhl H (1958) Toward the improvement of the quantitative phytoplankton method (German). *Mitteilungen International Verieningung fur Limnologie* 9:1–39.
14. Bargu S, Coale SL, Busman M, Doucette GJ, Silver MW (2002) Krill: A potential vector of domoic acid in marine food webs. *Mar Ecol Prog Ser* 237:209–216.
15. Miller PE, Scholin CA (1998) Identification and enumeration of cultured and wild Pseudo-nitzschia (Bacillariophyceae) using species-specific LSU rRNA-targeted fluorescent probes and filter-based whole cell hybridization. *J Phycol* 34:371–382.
16. Kleivdal H, Kristiansen SI, Nilsen MV, Briggs L (2007) Single-laboratory validation of the biosense direct competitive enzyme-linked immunosorbent assay (ELISA) for determination of domoic acid toxins in shellfish. *J AOAC Int* 90:1000–1010.
17. Kleivdal H, et al. (2007) Determination of domoic acid toxins in shellfish by biosense ASP ELISA—a direct competitive enzyme-linked immunosorbent assay: Collaborative study. *J AOAC Int* 90:1011–1027.

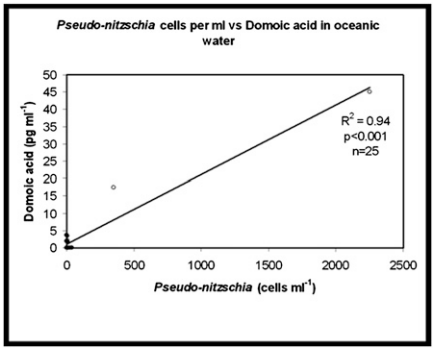

Fig. S1. The relationship between the number of intact (protoplast-containing) *Pseudo-nitzschia* cell numbers and domoic acid in ocean waters of the Pacific. *Pseudo-nitzschia* were identified by frustules shape and presence in characteristic stepped chains. Data are from all oceanic sites (Fig. 1 and Table S1).

Table S1. Complete data set of *Pseudo-nitzschia* abundances, DA cell quotas, DA levels in the water, and corresponding dissolved iron and nitrate concentrations

Cruise/ID	CTD station	Latitude	Longitude	Location	Fe, nM	NO_3, μM	*Pseudo-nitzschia* abundance, cells·L^{-1}	Cell quotas, pg·$cell^{-1}$	Water column DA, pg·L^{-1}
GOA /PT7	8	58.23N	142.16W	NE Subarctic Pacific	0.11	0.06	3.0×10^1	b.d.l.	b.d.l.
GOA/PT8	9	58.06N	142.52W	NE Subarctic Pacific	0.17	0.04	≤20	b.d.l.	b.d.l.
GOA/PT10	12	57.12N	143.13W	NE Subarctic Pacific	0.12	0.78	1.1×10^3	b.d.l.	b.d.l.
GOA /PT11	16	56.47N	143.2W	NE Subarctic Pacific	0.08	1.1	2.8×10^3	b.d.l.	b.d.l.
GOA /PT12	17	56.18N	143.45W	NE Subarctic Pacific	0.15	7.8	1.7×10^4	b.d.l.	b.d.l.
GOA /PT13	19	57.56N	142.44W	NE Subarctic Pacific	0.03	0.01	9.0×10^2	b.d.l.	b.d.l.
GOA /PT14	23	58.43N	144W	NE Subarctic Pacific	0.15	8.0	1.4×10^4	b.d.l.	b.d.l.
GOA /PT15	28	58.08N	147.51W	NE Subarctic Pacific	m.d.	m.d.	Present*	b.d.l.	b.d.l.
GOA/PT16	29	58.32N	148.12W	NE Subarctic Pacific	0.05	9.3	Present*	b.d.l.	b.d.l.
GOA/PT18	53	53.47N	155.2W	NE Subarctic Pacific	0.03	7.3	4.5×10^2	0.003	1.2
GOA/PT19	54	54.19N	155.32W	NE Subarctic Pacific	0.03	4.5	Present*	0.001	m.d.
GOA /PT20	55	54.59N	155.49W	NE Subarctic Pacific	0.04	16.5	3.6×10^3	0.0004	1.5
GOA /PT21	56	55.17N	155.55W	NE Subarctic Pacific	0.07	9.7	4.2×10^4	0.0003	12
GOA /PT22	57	55.3N	154W	NE Subarctic Pacific	0.01	6.3	Present*	b.d.l.	b.d.l.
GOA/PT23	58	55.14N	154.59W	NE Subarctic Pacific	0.04	3.6	8.0×10^2	0.0003	0.21
GOA/PT25	60	54.45N	156.59W	NE Subarctic Pacific	0.25	2.7	8.8×10^3	0.16	1.4×10^3
GOA /PT26	61	54.3N	158W	NE Subarctic Pacific	0.09	6.3	2.9×10^4	b.d.l.	b.d.l.
GOA/PT27	62, 63	53.39N	158W	NE Subarctic Pacific	m.d.	m.d.	1.7×10^3	b.d.l.	b.d.l.
VERTIGO ALOHA D1	19	22.79N	158W	Central Subtropical Pacific	m.d	0.2	b.d.l./20	m.d.	m.d.
VERTIGO ALOHA D1	27	22.76N	158W	Central Subtropical Pacific	m.d.	0.2	b.d.l./20	m.d.	m.d.
VERTIGO ALOHA D2	60	22.42N	158W	Central Subtropical Pacific	m.d	0.2	940/80	m.d.	m.d.
VERTIGO ALOHA D2	64	22.75N	159W	Central Subtropical Pacific	m.d	0.2	b.d.l./ 40	m.d.	m.d.
VERTIGO ALOHA D2	70	22.75N	157W	Central Subtropical Pacific	m.d	0.1	40/90	m.d.	m.d.
VERTIGO ALOHA D2	71	22.42N	157W	Central Subtropical Pacific	m.d	0.1	20/160	m.d.	m.d.
VERTIGO Aloha D2	79	22.75N	158W	Central Subtropical Pacific	m.d.	0.2	b.d.l./40	m.d.	m.d.
VERTIGO K2D1/ NT2	4,17,18, 25	47N	160E	NW Subarctic Pacific	m.d.	13.8	$3.0 \times 10^3/5.6 \times 10^3$	0.84	3.6×10^3
VERTIGO K2D1/ NT8	17, 18, 25, 28, 29	47N	160E	NW Subarctic Pacific	m.d.	13.6	$3.0 \times 10^3/5.6 \times 10^3$	0.40	1.7×10^3
VERTIGO K2D1/ NT9	17, 18, 25, 35, 36	47N	160E	NW Subarctic Pacific	m.d.	13.5	$3.0 \times 10^3/5.6 \times 10^3$	0.41	1.7×10^3
VERTIGO K2D2/NT12	76, 77	47N	160E	NW Subarctic Pacific	m.d.	12.6	$1.9 \times 10^3/1.2 \times 10^3$	1.9	3.6×10^3
IronEx II /240	240	3.55N	104W	Equatorial Pacific	0.24	7	2.3×10^6	0.2	4.5×10^4
IronEx II /331	163	3.55N	104W	Equatorial Pacific	0.08	8	3.5×10^5	0.5	1.8×10^4
SOFeX /36 (South)	19	66S	172W	Antarctic Pacific	0.06	25.8	2.0×10^3	1.0	2.0×10^3
SOFeX /40 (South)	23	66S	172W	Antarctic Pacific	0.15	25.0	3.0×10^3	0.69	2.1×10^3
SOFeX /29 (South)	29	66S	172W	Subantarctic Pacific	0.06	25	2.2×10^5	1.0†	2.2×10^5
SOFeX /45 (North)	45	53S	167W	Subantarctic Pacific	<0.04	19	3.7×10^5	m.d.	m.d.

The table presents data for all samples that were examined for *Pseudo-nitzschia* and DA in the present study. "Cruise/ ID" indicates the oceanographic expedition on which the sample was obtained and the sample ID. "GOA" indicates the Gulf of Alaska cruise, and "b.d.l." indicates measurements were below detection limits of our methods; for cell counts, the detection limit in water samples was 20 cells·L^{-1} in the water. Generally, DA cell quotas of ≤1 fg·$cell^{-1}$ were difficult to detect, given the abundance of other species in the samples. (See comments in Table 1 for the term "b.d.l." when used for DA cell quotas.) The designation "m.d." indicates missing data: Samples were either unavailable for counting or DA was not measured due to the low abundance of *Pseudo-nitzschia* cells (i.e., sufficient cellular material as required for the cELISA would have been unattainable, e.g., VERTIGO ALOHA). Generally, *Pseudo-nitzschia* abundances were estimated from cell counts made from surface (10–30 m) water samples that corresponded to net tows taken for the DA samples. For VERTIGO ALOHA, two values are given for *Pseudo-nitzschia* abundances (e.g., 940/80). These values represent cell densities from two discrete depths (25 m/125 m) within the euphotic zone (125 m). Likewise, two depth values are given for VERTIGO K2 (euphotic zone depth of 60 m); cell abundances from 10 and 40 m. "D1" and "D2" indicate trap deployment periods during which water samples were collected for cell abundances and *Pseudo-nitzschia* standing stocks. These data were then integrated over the depth of the euphotic zone at each site (160 m for ALOHA, 60 m for K2) to calculate the standing stock of *Pseudo-nitzschia*. DA cell quotas were calculated from DA measurements on concentrated net tow samples corresponding to the water samples counted for abundances in that same sample.

*"Present" indicates that counts were not made but *Pseudo-nitzschia* cells were observed in water samples (*SI Methods*).

†For SOFeX South, Station 29, there was no corresponding measurement of cellular DA (i.e., no sample was available), so we used the value from station 36 that was taken 2 d later at the same location as station 29 to calculate 220 ng·L^{-1}.

Table S2. Morphometrics of *Pseudo-nitzschia* found at oceanic stations in this study

Species	Length, μm		Width, μm		Striae in 10 μm		Fibulae in 10 μm		Poroids in 1 μm		Rows of poroids	Central interspace	Location	Cruise
	Min	Max	Min	Max	Min	Max	Min	Max	Min	Max				
P. cuspidata	34	36.7	1.4	1.5	30	31	19	19	5	6	1 or 2	Present	Equatorial Pacific	IronEx II
P. delicatissima	38	65	1.8	2.2	32	34	16	20	6	8	2	Present	Equatorial Pacific	IronEx II
P. fraudulenta	82.4	82.4	3.1	3.1	22	22	14	14	8	8	2	Present	NE Subarctic Pacific	GOA
P. granii	>35		1.3	1.3	32	32	13	13	5	6	1	Present	NE Subarctic Pacific	GOA
	86	86	1.48	1.48	48	48	14	14	6	7	1	Present	Antarctic Pacific	SOFeX (South)
P. heimii	70.3	86	1.8	2.9	22	28	12	16	7	10	2	Present	NE Subarctic Pacific	GOA
	72	82	2	3.7	24	30	19	22	8	9	2	Present	Equatorial Pacific	IronEx II
P. inflatula	46.3	46.3	2.7	2.7	36	36	20	20	6	6	1	Present	NE Subarctic Pacific	GOA
	36.7	36.7	1.5	1.5	30	30	19	19	5	6	1 or 2	Present	Equatorial Pacific	IronEx II
P. lineola	85	86.4	2.4	2.9	20	22	12	14	8	8	2	Present	NE Subarctic Pacific	GOA
	75	80	2.3	2.3	27	27	16	16	4	5	1 or 2	Present	Equatorial Pacific	IronEx II
	55	110	1.6	2.2	21	26	10	16	3	7	1	Present	Antarctic Pacific	SOFeX (South)
P. pseudodelicatissima	63	109	1.84	2.5	22	32	14	18	4.6	8	1 or 2	Present	NE Subarctic Pacific	GOA
	81	81	2.1	2.1	21	21	11	11	3	4	1	Present	Antarctic Pacific	SOFeX (South)
P. roundii	77	101.9	4.7	5.5	31	36	18	20	5	5	1	Present	Equatorial Pacific	IronEx II
P. turgidula	65.7	70.1	2.2	3	21	23	14	14	7	8	1 or 2	Present	NE Subarctic Pacific	GOA
	52	75	1.8	2.1	19	30	13	24	8	10	1 or 2	Present	NW Subarctic Pacific	Vertigo K2
	130	140	2.9	2.9	20	22	19	19	6	7	2	Present	Equatorial Pacific	IronEx II
P.cf turgiduloides	>36	—	2	2	20	20	10	10	4	5	1	—	Antarctic Pacific	SOFeX (South)

Dimensions are shown for the various silica valve features of the 11 species found in the 12 samples examined by electron microscopy (SEM and TEM). These dimensions fall within the size ranges reported for those species in the literature. "Location" refers to the oceanic regions where the species was encountered and "cruise" refers to the expeditions/sites in the present study.